A DEEP LEARNING CNN APPROACH WITH UNIFIED FEATURE EXTRACTION FOR BREAST CANCER DETECTION AND CLASSIFICATION

By

ONGOLE GANDHI * TIRUMALA RAO S. N. ** MUNAGA H. M. KRISHNA PRASAD ***

*,*** Department of Computer Science and Engineering, Jawaharlal Nehru Technological University, Kakinada, Andhra Pradesh, India.
** Department of Computer Science and Engineering. Narasaraopeta Engineering College, Narasaraopet, Andhra Pradesh, India.

https://doi.org/10.26634/jip.12.2.21915

Date Received: 23/04/2025 *Date Revised: 22/05/2025* *Date Accepted: 25/06/2025*

ABSTRACT

Radiologists typically have a hard time to classify the breast cancer, which leads to unnecessary biopsies to remove suspicions, and this ends up in adding exorbitant expenses to an already burdened patient and health care system. As well as early detection and diagnosis can save the lives of cancer patients. In this paper, a computer-aided diagnosis (CAD) system based on hybrid intelligence framework using Gabor wavelet-based deep learning convolutional neural network (GW-DL-CNN) for the detection and classification of breast cancer in mammographic images is proposed. In addition, a machine learning framework with Gabor wavelet-based support vector machine (GW-SVM) also implemented. Both, GW-SVM and GW-DL-CNN models are proposed to help the radiologist in a much better way to detect and classify the breast cancer from mammographic images. Further, Chan-Vese (C-V) features-based level set segmentation also utilized for segmenting the objects without clearly defined boundaries in mammographic images. The unified features extracted from C-V and GW are fed into an architecture of DL-CNN to classify the type of breast cancer such as malignant, benign, or normal using fully complex valued relaxation network (FCRN) classifier. The proposed frameworks of GW-SVM, GW-DL-CNN with FCRN classifier is achieved the model accuracy of 98.6%, specificity of 98%, sensitivity of 98% and F1-Score is 97.08% respectively.

Keywords: Mammographic Imaging, Breast Cancer, Segmentation, Gabor Wavelet, Deep Learning, CNN.

INTRODUCTION

Cancer is an unwelcome cell with peculiar characteristics that varies from normal breast tissue cells. This develops into cancer, which affects both men and women, spreads quickly, invades nearby tissue, and forms. The major cause of malignancies in women that contribute to an increase in mortality is now breast cancer. Since the early 1990s, there has been a decline in breast cancer-related deaths, with younger women under 50 seeing bigger drops. The ratio has decreased as a result of early cancer discovery through screening, which has also enhanced and raised women's knowledge of the disease. The breast duct is where cancer cells typically first appear, followed by the lobule area, and in a very small percentage of instances, the tissues surrounding the breast region. Approximately 80% of women are diagnosed with invasive ductal carcinoma, a kind of breast cancer that has progressed to the tissues around the breasts (Sebai et al., 2020; Zheng et al., 2020). Breast cancer frequently begins in the duct area, spreads by breaching the duct wall, and eventually reaches the fatty tissues, increasing the disease's aggressiveness. Sometimes the lymph node served as a conduit for the malignant cells to ultimately spread to other places of the body. This forces the clinical person to undergo screening in order to identify and diagnose cancer early (Chavez et al., 2019; Wang et al., 2020a). To improve the survival rate of people, it is necessary to take appropriate prognostic measures to prevent breast removal, the side effects of chemotherapy, and the effects of radiation treatment. Breast images with the highest level of accuracy to be used to identify the destructive malignant tissue since human life is at stake. In order to discover the malignancy and reduce erroneous predictions, computer-aided detection is employed as an examination approach (Huang et al., 2019; Valkonen et al., 2019). This technique simply involves reading the picture again for the radiologist to acquire more clarity. Therefore, creating a computer-aided tool to assist oncologists has grown to be of significant interest. Breast images are acquired using a variety of imaging modalities, and they are then converted to allow for additional analysis and the extraction of picture attributes. The specialized tissues in a woman's breast that make milk might include fatty tissues. It results in an abnormal arrangement that multiplies and divides uncontrollably, which frequently accelerates the development of cancer (Eltrass & Salama, 2020; Roslidar et al., 2020; Wang et al., 2019). Breast cancer starts in the gland cells and spreads to the milk ducts. The statistical data for breast cancer in India is shown in Figure 1, and it can be seen that women between the ages of 30 and 50 have a higher risk of developing the disease. And due to the advancement in technologies, for every 25 years cancer detection is reducing, but still, it needs to improve more. Thus, by performing the accurate detection and

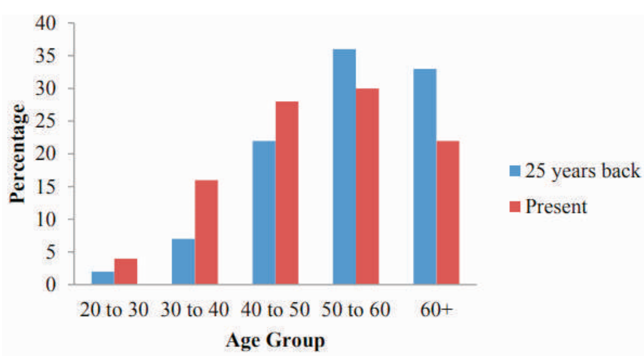

Figure 1. Indian Breast Cancer Statistics

classification methods breast cancer problems will be overcome in India. To achieve this, various researches are contributed their work, and proposed the variety of methodologies. Lotfi and Keshavarz (2014) used machine learning processes and soft computing approaches for assessing the breast lesion picture in order to detect the various types of breast lesions using an intelligent automated methodology. Principal component analysis (PCA) is used in this case to distinguish between melanoma breast lesions. This method is also used for preprocessing, and optimization is completed using soft computing.

The novel, enhanced Random Forest-based Rule Extraction (IRFRE) approach was employed for classification operations (Wang et al., 2020b). The primary goal of this effort is to choose correct characteristics to create a breast cancer detection system with little mistake. The goal of combining an analytical technique and segmentation method is to improve these two strategies and provide a diagnostic process interface. Adem (2020) utilized the K-nearest neighborhood (KNN) method for classification of breast cancers. Here the subspace based KNN algorithm is proposed in combination with the stacked auto encoders. But this approach is failed to provide the maximum accuracy due to inconsistency of KNN with SAE, respectively. Banu and Thirumalaikolundusubramanian (2018) proposed the various methods of transfer learning approaches using the various types of naïve Bayes classifiers for efficient detection of classification. This method shows, the better way to provide the hybrid approaches. For classification, this study suggested the Bayes belief network (BBN), boosted augmented naive Bayes, and tree augmented naive Bayes networks. But this method provides the high false rates as this method do not support the high level of training. To solve the database training problems, SVM-based training and testing can be suitable perfectly. Vijayarajeswari et al. (2019) suggested Hough transform based feature extraction with SVM for classification. However, the hog features can extract only the local features, but these features are insufficient for the classification, thus it leads to improper classification and results in poor accuracy. An Extreme Learning Machine-based classification model was developed by efficiently leveraging the Radial Basis Function (RBF) kernel to address the issues associated with SVM classification (Mojrian et al., 2020). The RBF kernel can effectively classify the two types of cancers, but this method failed to provide the linear properties.

To reduce the constraints related to classification problems, several studies investigated optimization algorithms such as Artificial Bee Colony feature selection, Particle Swarm Optimization (PSO), Binary Whale Optimization, and the Chaotic Salp Swarm Algorithm, in addition to machine learning classification (Melinda et al., 2020; Utami & Rustam, 2019; Sayed et al., 2020; Ibrahim et al., 2020). But the major drawbacks of these optimization algorithms are lies in enhancement of accuracy in forceful manner. In addition, these optimization algorithms increase the classification accuracy by training the system with only specified recognized features. To solve these problems, self-optimization-based fuzzy inference systems were introduced (Li & Fong, 2023). But the fuzzy models are rule based approaches and can train the systems with maximum accuracy but at the cost of high computational complexity. Later artificial intelligence based deep learning approaches introduced for classification operation. Kaymak et al. (2017) proposed the artificial neural network (ANN) approach for detection of breast cancer with radial basis neural networks model. This method provides the less classification accuracy is it is consisting of low-level layered architecture.

Pérez et al. (2017) developed the texture feature based back-propagation neural networks for efficient detection of the breast cancers. These back-propagation models increase the accuracy by feed backing the data through error resilient manner. Although the genuine positive rate is increased by this back-propagation process, the false positive rate is also increased. Hence, the statistical parameters sensitivity and specificity of the systems reduces due to neural network feedbacks. Sujatha et al. (2020) developed the ANFIS approach for detection of breast cancer, which combines the ANN system with FIS rules. This method utilized the texture-based features for classification, so it results in an additional optimization of features or requires the hybrid features. Genetic algorithms and ant colony optimization in combination with the ANN-ANFIS system were used to address these problems (Bilalović & Avdagić, 2018; Thangavel & Kaja Mohideen, 2016). To solve the problems of ANNs, the deep learning based neural networks are introduced. Nahid et al. (2018) introduced the deep neural networks for classification. However, this method is failed to provide the segmentation accuracy with low level classification. Ting et al. (2019) suggested the CNN for classification of breast cancer with the usage of multiple combination of layers. However, these layers made the system complicated and not supported to all the types of features. To solve this, a hybrid DL-CNN mechanism was formed by combining recursive neural networks (RNNs) with CNNs (Yao et al., 2019). However, RNNs still have time complexity issues, such as longer training times and delays in obtaining classification outcomes. Hu (2020) developed, pulse coupled neural network-based detection and classification of breast cancers, which is an iterative approach, thus it needs the large amount of testing data sets. But this system is not effective for low resolution input images. Budak et al. (2019) proposed the bidirectional long short-term memory (Bi-LSTM) and fully convolutional model for the detection and classification of breast cancer. However, the major drawbacks of DL-based systems in the literature are, most of them are focused only on the classification part and omitted the segmentation features and texture feature extraction approaches, separately. Duraisamy and Emperumal (2017) introduced the advanced hybrid DL-CNN approach with C-V level set segmentation with feature extraction is implemented. However, they have not considered texture feature extraction which led to inaccurate detection of regions. Therefore, to further enhance the classification accuracy, the DL-CNN approach needs additional texture feature extraction strategies with modified layered architectures. In addition, preprocessing of mammographic images like cropping, extraction of region of interest and normalization are also important to extract the texture features. The following contributions of this research are as:

- Implementation of a novel Computer-Aided Diagnosis (CAD) system for breast cancer detection using GW-SVM, integrated with Chan-Vese segmentation to accurately segment objects with poorly defined boundaries in mammographic images.
- In addition, the performance of the proposed GW-SVM is evaluated and shown to outperform existing CAD systems for breast cancer detection and classification, including IRFRE, SAE + KNN, TAN Bayes, and Hough + SVM (Wang et al., 2020b; Adem, 2020; Banu & Thirumalaikolundusubramanian, 2018; Vijayarajeswari et al., 2019).
- Furthermore, a hybrid DL-CNN model utilizing unified features extracted from Chan-Vese (C-V) and GW methods, combined with an FCRN classifier, is implemented to address the limitations of existing deep learning-based approaches for breast cancer detection, such as ANN, CNNI-BCC, DL-CNN + NN, and Level Set + DL-CNN + NN (Kaymak et al., 2017; Ting et al., 2019; Duraisamy & Emperumal, 2017).

1. Proposed Methodology

Figure 2 shows the detailed architecture of the proposed methodology for breast cancer detection and classification. The process begins with the acquisition of a mammogram image, which is then subjected to a pre-processing stage. This stage involves the removal of irrelevant background region through a cropping technique, extraneous parts of the mammogram are subsided, and a focused Region of Interest (ROI) in the mammogram is identified. Subsequently, a normalization procedure is applied to the ROI to remove the noise and enhance the visibility of diagnostic, significant features. After preprocessing, Chan–Vese segmentation algorithm is employed to accurately detect and delineate cancer-affected areas within the ROI. The resulting segmented image is then used for feature extraction using two complementary approaches: the Chan–Vese (C-V) feature method and the Gabor-Wavelet (GW) filter method. The C-V method extracts features related to image contours and edges, while GW extracts features related to texture and local frequencies. Then the unified features extracted from the C-V and GW methods are independently passed through two parallel classification pathways: a Support Vector Machine (SVM) and a Deep Learning–based Convolutional Neural Network (DL-CNN). These components are highlighted in orange. The SVM operates as a conventional classifier to categorize the mammogram as malignant, benign, or normal based on the extracted features. In parallel, the DL-CNN employs a fully complex valued relaxation network (FCRN) classifier in place of the traditional fully connected layer. The detailed operation of each block is described as follows:

1.1 Pre-processing

Generally, the mammogram images contain the unwanted regions such as labels. Thus, it is necessary to remove the noise affected or unwanted regions to increase the detection accuracy which results in

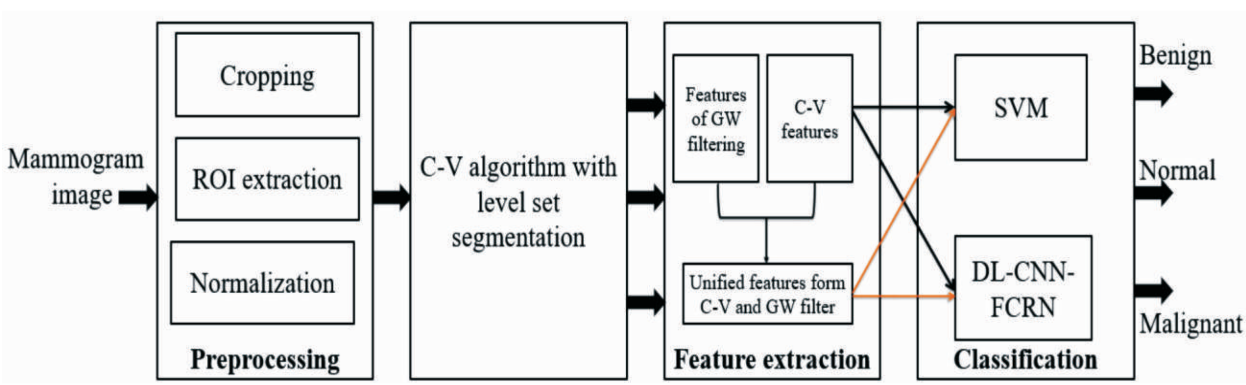

Figure 2. Proposed Architecture of Breast Cancer Detection and Classification Using GW-SVM and GW-DL-CNN Models

improved accuracy in classification. A deeper look at the mammograms indicates a number of challenges with the diagnosis. The preprocessing approach may be used to prevent differences in the overall look, such as brightness, contrast, and other visual characteristics, of the breasts, which are frequently caused by variances in the image capture process.

1.1.1 Cropping

The Region of Interest (ROI) is extracted by applying the bounding box method. Images are explicitly rescaled to maintain the aspect ratio after being cropped to the bounding box of the lesions.

1.1.2 ROI Extraction

The ROI extraction method uses both a region-based and a thresholding-based approach. Geometrically, ROI is a 2-dimensional plane that divides the cancer-affected pixels from the surrounding pixels. The foreground and background are presumed to be black, while the transitional zones are thought to be white. The transition zones really demarcate the foreground from the backdrop. The following three requirements should be met by the ROI extraction:

- Transition area has a higher density of pixels close to non-step edges than other regions do, which have a higher density of pixels close to step edges.
- Boundary property surrounds the item and is situated between object and backdrop.
- Variation in gray levels refers to the general tendency of gray levels in the transition area to shift frequently and intensely, providing a wealth of descriptive data; however, gradient-based methods are noise-sensitive and more appropriate for brief, sharp level changes than for more regular gray level changes. Numerous local statistics-based alternatives were created to get around this restriction. For the purpose of extracting the transition area, the local ROI statistics such as local entropy, modified local entropy, and gray level difference are used.

1.1.3 Normalization

The extracted ROI is applied as an input to the normalization process. The pictures are normalized by projecting all mammography images into a predefined intensity range among r1 and r2 (0 < r1 < r2 < 255). In order to limit the variance and establish computational consistency. Think of the ROI extracted picture g_s (x,y) as having a maximum gray level value of g_{max} and a minimum gray level value of g_{min}. Consequently, normalization may be defined as Equation 1.

$$I_n(x,y) = r1 + \frac{[\, g_s(x,y) - g_{min}.(r2 - r1)]}{g_{max} - g_{min}} \quad (1)$$

Due to the fact that maximum intensities and minimum intensities of the microcalcifications are not, with certainty, above r2 and below rl after examining a large number of mammograms, rl and r2 are given the values 60 and 210 in this case.

1.2 C-V Level Set Segmentation

Segmentation of an image referred as dividing an image into its constituent regions and separation of the cancer affected region from the background. For this purpose, C-V level set segmentation method provides the level set implementation of C-V model and its solution by active contour approach. Consider normalized output image I_n with ROI which is denoted as R. The principal purpose of the model is to minimize the energy function (Equation 2).

$$E(c_1, c_2, C) = v.Length(C) + \sum_{i=1}^{2} \int (I_n(x,y) - c_i)^2 dxdy \quad (2)$$

Where v is a level set constant, c_i such as c_1 and c_2 represents inside and outside regions of active contour C, which also indicates the interior and exterior intensity values of C. The level set function, also known as the Lipschitz function (∅), which is used to depict the contour C as C = {(x, y) | ∅ (x, y) = 0}. Zero level curves at time t of the function ∅ (t, x, y) are used to illustrate the development of the curve (Equations 3 - 5).

$$C = \{(x,y) | \emptyset(x,y) = 0\} \quad (3)$$

$$\Omega_1 = \{(x,y) | \emptyset(x,y) > 0\} \quad (4)$$

$$\Omega_2 = \{(x,y) | \emptyset(x,y) < 0\} \quad (5)$$

Here, Ω_1, and Ω_2 are the C-V level set parameters over the total range Ω.

Equation 6 define the Heaviside function as:

$$H(z) = \begin{cases} 1 \ \ if \ z \geq 0 \\ 0 \ \ if \ z < 0 \end{cases} \tag{6}$$

The energy of level set function $\varnothing$ in level set form can be rewritten as Equation 7.

$$E(c_1, c_2, \phi) = v\int_{\Omega}^{\cdot} |\nabla H(\phi)| dxdy + \int_{\Omega}^{\cdot} I_n(x,y) - c_1)^2 H(\phi) dxdy + \int_{\Omega}^{\cdot} (I_n(x,y) - c_1)^2 (1 - H(\phi)) dxdy \tag{7}$$

The segmentation contour is extracted by minimizing the Equation 7 with respect to $\varnothing$. The minimized value obtained using gradient descent approach yields (Equation 8).

$$\frac{\partial \emptyset}{\partial x\, \partial y} = \delta(\emptyset) \left[v.\, div\left(\frac{\nabla_{\emptyset}}{|\nabla_{\emptyset}|}\right) - (I_n(x,y) - c_1)^2 + (I_n(x,y) - c_2)^2 \right] \tag{8}$$

Where $\delta(\varnothing)$ is the Dirac function and solved using Euler–Lagrange equations.

The solutions of Equation 9, generates the segmented output image C(t), which acts as a boundary between two sets $\{(x, y) | I_n \approx c_1\}$ and $\{(x, y) | I_n \approx c_2\}$. The solution is provided by semi-implicit gradient descent approach where the image is sampled on a regular grid $\Omega = \{0, \ldots, M\} \times \{0, \ldots, M\}$.

$$C(t) = Region[\ \{(x,y)| f \approx c_1\}, \{(x,y)| f \approx c_2\}\ ] \tag{9}$$

1.3 Feature Extraction

The performance of classification directly depends upon the features used to represent the segmented image. The feature should provide the maximum amount of information about segment image, with minimum number of feature vectors. The extracted features have the property of invariance and re-constructability. The invariance property implies that the extracted features must remain unchanged even if the input image undergoes some transformations like translation, rotation and scaling. On the other hand, the reconstruct property is exactly the reverse of feature extraction, where image is regenerated from the extracted features. This characteristic makes sure that the retrieved features accurately reflect the mammographic picture shape. While not always attainable, reconstruct ability is a desirable property. The feature extraction methods can be classified as structural and statistical. These structural features are concentrated on small and region of image; therefore, their extraction from the image requires careful processing. Statistical features can be detected more easily and are not as sensitive to local noise or distortions as are structural features. In this work, the feature extraction methods namely C-V features and GW features are utilized.

1.3.1 C-V Based Segmentation

Figure 3 shows the C-V segmentation technique is used to separate objects without clearly defined borders. This algorithm is built on level sets that are iteratively evolved to minimize an energy that is defined by weighted values corresponding to the sum of differences in intensity from the average value outside the segmented region, the sum of differences from the average value inside the segmented region, and a term that depends on the length of the segmented region's boundary.

C-V level set features were extracted from the input segmented mammogram in three steps: level set features computation from normalized image, directional decomposition, and feature down sampling.

Consider a normalized segmented image position I(x,y) of dimensions M×N and the level set vector L(x,y) is evaluated at each pixel position I(x,y) by applying sobel operator. The two components are computed as Equations (10, 11).

$$L_x(x,y) = I(x+1, y-1) + 2I(x+1, y) + I(x+1, y+1) - I(x-1, y-1) - 2I(x-1, y) - I(x-1, y+1) \tag{10}$$

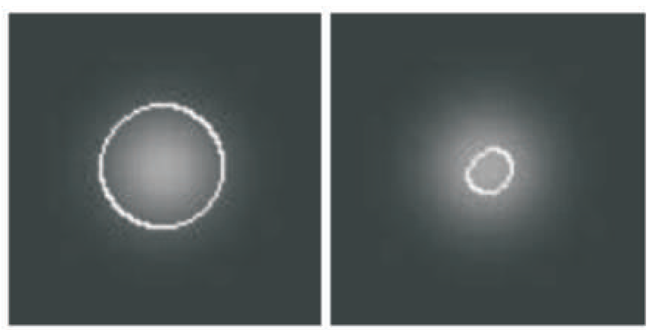

(a) (b)

Figure 3. Segmentation Results Comparison (a) Segmentation Using C-V Method (left). (b)Segmentation Using Gradient-based Method (right)

$$L_y(x,y) = I(x-1,y+1) + 2I(x,y+1) + I(x+1,y+1) - I(x-1,y-1) - 2I(x,y-1) - I(x+1,y-1) \quad (11)$$

Where L_x (x,y) and L_y (x,y) represents the horizontal and vertical level set components, respectively. These level set components are used to compute the directions and magnitude (strength) of level set vector L (x,y) using Equations (12, 13).

$$Magnitude = |L(x,y)| = \left(L_x^2(x,y) + L_x^2(x,y)\right)^{\frac{1}{2}} \quad (12)$$

$$Direction = arg\left(L(x,y)\right) = \tan^{-1}\left(L_y(x,y)/L_x(x,y)\right) \quad (13)$$

The direction of level set vector is not along any of the discrete directions; therefore, it is decomposed into two component vectors V_1 and V_2 which lies along discrete directions. The strengths of component vectors correspond to directional images I1(x,y) and I2(x,y). On the other hand, if the direction of level set vector is along one of the discrete directions, then the strength of vector is assigned to corresponding sub image only. The directional decomposition results in 8-directional sub images I_d (x,y),d=1,2,.......8 hold the level set features.

1.3.2 Gabor-wavelet Features

The GW filter consists of sinusoidal/harmonic function modulated by Gaussian distributions. The functions used in 1-dimensional filter can be extended to two dimensions to create filters which are selective for orientations. The advantage of using GW filters lies in the fact that they are less sensitive to noise and show some degree of invariance towards several transformations like translation, intensity, and orientation. A two-dimensional GW filter is defined as Equations (14 - 17).

$$f(x,y,\theta_k,\ ,\sigma_x,\sigma_y) = \exp\left[-\frac{1}{2}\left\{\frac{R_1^2}{\sigma_x^2} + \frac{R_2^2}{\sigma_y^2}\right\}\right] * \exp\left(i\frac{2\pi R_1}{\gamma}\right) \quad (14)$$

Where, $\exp\left[-\frac{1}{2}\left\{\frac{R_1^2}{\sigma_x^2} + \frac{R_2^2}{\sigma_y^2}\right\}\right]$ represents the Gaussian envelop,

and $\exp\left(i\frac{2\pi R_1}{\gamma}\right)$ is the complex harmonic plane.

Here $\quad R_1 = x\cos\theta_k + y\cos\theta_k \quad (15)$

$$R_2 = -xsin\theta_k + ycos\theta_k and\ exp\left(i\frac{2\pi R_1}{\gamma}\right) = cos\left(\frac{2\pi R_1}{\gamma}\right) + \text{i}\sin\left(\frac{2\pi R_1}{\gamma}\right) \quad (16)$$

The parameter γ represents the wavelength of the harmonic plane, or inversely the frequency of the plane. The large wavelength responds to gradual changes in the image intensity, and the short wavelengths respond to edges. The parameter θ_k specifies the orientation of complex harmonic plane. The value of θ_k varies from 0 to 2π, as angles from are not assumed because of symmetry of the plane. The standard deviations of Gaussian envelop along x-axis and y-axis is denoted by σ_x and σ_y and indicates the spread of 2-dimensional Gaussian function. In this work, the Gaussian function is considered with $\sigma = \sigma_x = \sigma_y$. This value also determines the extent of image which affect convolution.

$$R_2 = -xsin\theta_k + ycos\theta_k and\ exp\left(i\frac{2\pi R_1}{\gamma}\right) = cos\left(\frac{2\pi R_1}{\gamma}\right) + isin\left(\frac{2\pi R_1}{\gamma}\right) \quad (17)$$

Theoretically the whole image should be involved in convolution, therefore the value of is typically assumed to be proportional to the wavelength of the harmonic plane. The rotation of complex harmonic plane by angle θ_k results in GW filter for orientations of θ_k. The orientations are evaluated by using $\theta_k = \frac{\pi(k-1)}{m} \forall k = 1,2,\ldots.m$ where k represents the total number of orientations of harmonic plane. The GW features are the response of GW filter on the image. The features are obtained by convolving the image with GW filter. If I (x, y) denotes the image, then the convolution of image with GW filter is given by Equation 18.

$$G(x, y, \theta_k, ,\sigma) = I(x, y) * f(x, y, \theta_k, \gamma, \sigma) \quad (18)$$

Where $G(x, y, \theta_k, \gamma, \sigma)$ is GW representation of image I (x, y).

Generally, feature vectors are computed by taking the square root of real part and imaginary part of the filter response. To evaluate the GW features, initially the input images are normalized to 32×32. The GW filter is convolved with whole image for different orientations. These orientations have been chosen by evaluating the performance of filter for different number of orientations. The performance is computed by using 5-fold cross validation on the dataset. Therefore, 9 orientations of the complex plane are considered, namely 0, $\pi/9$, $2\pi/9$, $3\pi/9$, $4\pi/9$, $5\pi/9$, $6\pi/9$, $7\pi/9$, $8\pi/9$. For each value of orientation, the collective values of real and imaginary components are used to evaluate the feature values. Hence a total of nine feature values corresponding to all orientations are evaluated. GW features are also evaluated by partitioning the whole image into quadrants and sub quadrant. Each partition of the image also contributes nine features to the feature set resulting in 189 ($1\times9 + 4\times9 + 16\times9$) feature values. The number of feature values can be increased or decreased by varying the number of orientations of the complex plan.

1.4 Classification

1.4.1 GW-SVM Classification

SVM is a supervised learning-based binary classifier. Using the hyper plane to provide decision boundaries for dividing the data points into distinct classes is the core idea behind SVM. The SVM's fundamental principle is to divide data into two categories by building a hyperplane in a high-dimensional feature space. The SVM uses a nonlinear function loaded with GW features to translate the d-dimensional input vectors from input space to high dimensional feature space. The definition of the separating hyper plane is $W^T \varphi(X_i) + b = 0$, where W is a weight vector of dimension $\varphi(x)$ and b is a bias. When the data are linearly separable, there are several approaches to determine the separating hyper plane. The goal of SVM, which is based on the maximum margin concept, is to build a hyperplane by meeting the maximum distance between the cancer classes.

$$W^T \varnothing(X_i) + b \geq +1 \text{ for } Y_i = +1 \quad (19)$$

$$W^T \varnothing(X_i) + b \leq -1 \text{ for } Y_i = -1 \quad (20)$$

$$Y_i(W^T \varnothing(X_i) + b) \geq 1, I = 1, 2, \ldots\ldots, n \quad (21)$$

Equation (19), and Equation (20) represents the class values and Equation (21) represents the multi-class mathematical model.

Finally, the classifier is defined as Equation 22.

$$F(X_i) = \text{sign}(W^T \varnothing(X_i) + b) \quad (22)$$

The function returns $F(X_i) \geq 0$ for $Y_i = +1$ and $F(X_i) \leq 0$ for $Y_i = -1$ for each training set of data X_i. Support vectors are components of the training dataset that are located near the intersection of the hyperplanes for the two classes. Before using training data in SVM, the kernel's parameters must be changed. The Gaussian radial basis function is found to be the best kernel after testing a variety of kernel functions throughout the simulations. The training datasets comprise benign, malignant, and normal subsets that aid in classifying the test picture as a normal, benign, or malignant malignancy during the classification phase. Proposed GW-SVM classification algorithm is shown below.

Input: Segmented image 'I', Training data X_i

Output: Classified image, 'S' {S = 1 for benign, S = -1 malignant}

Step 1: W initialize the weight

Step 2: Update the bias value

Step 3: update the kernel with Gabor wavelet feature $\varphi(X_i)$

for (i = 1 to size (I))

for (j = 1 to size (X_i))

Step 4: $F(X_i) = \text{sign}(W^T \varphi(X_i) + b)$

end for j

end for i

Step 5: Generated the classification outcome by probability distribution

$$S = \begin{cases} 1, & F(X_i) \geq 0 \\ -1, & F(X_i) \leq 0 \end{cases}$$

1.4.2 GW-DL-CNN Integrated with FCRN Classification

The GW-DL-CNN feature learning methods identify the common patterns that are crucial for differentiating across classes and automatically extract them for use in regression or classification. Hierarchical architectures are used in DL methods. Especially with non-linear image processing which consist of numerous stages. These are used for feature learning and pattern categorization. It offers doctors and other medical personnel strong diagnostic help. It makes an effort to understand various representational and abstract levels that aid in automatically making sense of data. A hierarchy of nonlinear characteristics with increasing complexity is formed by convolutional layers in deep learning (DL), which are exceptionally effective at identifying salient patterns in pictures. The pooling approach reduces the amount of memory used. As a result, it permits the use of more convolutional layers. In the last step, categorization is done using all of these created characteristics. There are so many processing levels exist in this kind of neural network. It comprises of 2 layers: First, convolutional layer and second is nonlinear sub sampling layer. The picture is subjected to filters in convolutional layers, and a subsampling layer reduces the input size of the image. It is followed by a multinomial logistic regression layer and numerous fully linked layers.

Calculate the yield at position j from the input for the convolutional layers (Equations 23 - 25). using the bias and filter b_k, W_k (at the k^{th} level),

$$X_k(j) = \sigma\left(\sum_{i\in(j)} X_{k-1}(i) * W_k(i,j) + b_k(j)\right) \quad (23)$$

Where, σ(.) denotes rectification linear unit (ReLu) function, Ω (j) denotes input picture, and * stands for the convolution operator. The non-linear sub sampling layers is defined as:

$$X_k(j) = \downarrow X_{(k-1)}(j) \quad (24)$$

Where, ↓ (.) stands for a sub sampling function that sum up input image's area data which defines as Ω(j). Multinomial logistic regression layer uses the variables X_L from the L^{th} layer. The probability of the i^{th} class is determined with function SoftMax and it is defined as:

$$y(i) = \frac{e^{X_L(i)}}{\sum_j e^{X_L(j)}} \quad (25)$$

The stochastic gradient descent approach is used for training. This training uses feed-forward fashion approach to reduce the cross-entropy loss. The mammography pictures are classified using an FCRN classifier in the final step. The FCRN classifier has received the features that were retrieved from the DL framework as input. Because it is more generalizable than previous networks. In this study, neural network based complex-value network is preferred. It is suggested to utilize a single hidden layer neural network with a completely complex value and a hidden layer activation function that is similar to a hyperbolic secant function for a Gaussian search. In this architecture, the output layer is particularly using an exponential activation function. The network parameters are calculated using a projection-based learning technique. This method solves a system of linear equations and estimates optimal output weights. Since any desired function may be approximated with little computing effort, higher precision is possible. By using circular transformation, input characteristics with the real values are translated to compound domain. All four quadrants of the complex domain are mapped 1:1 from the real-valued input characteristics. As a result, the FCRN classifier's orthogonal decision bounds are fully used. Due of the density and variety of suspicious regions in digital mammograms, the FCRN classifier is used among any other classifier with the capability of learning. Figure 4 shows the architecture of DL-CNN with FCRN classifier, which employs the combination of GW and C-V level set hybrid features. From this approach, sufficient amount of information is extracted with the help of proposed combination. This aids in classifying the pixels with belongs to different breast tissues with high accuracy. Convolutional layers, ReLU activation layers, max pooling layers, and fully linked layers are the first three phases of this architecture.

1.4.3 DL-CNN Architecture

The suggested DL-CNN with FCRN classifier is generally described as follows:

- Input mammogram with size [128 x 128 x 3] stores the picture's raw pixel values; in this instance, an image with a width of 128 pixels, a height of 128 pixels, and three-color channels (R, G, and B).
- The CONV1 layer computes the output of neurons linked to local areas in the input, with each neuron calculating a dot product between its weights and the local region in the input volume to which it is connected. This might result in the usage of 32 filters and a volume of [128 x 128 x 32].
- An element-wise activation function, such as the max (0, x) thresholding at zero, is applied by the RELU1

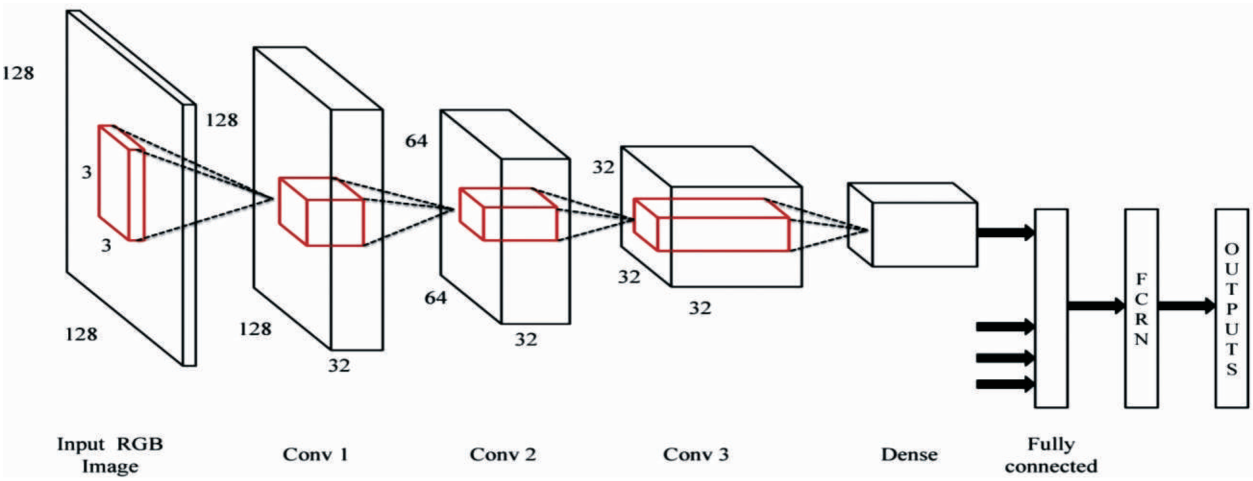

Figure 4. Architecture of the Deep Learning CNN Integrated with FCRN Classifier

layer. As a result, the volume's dimensions [128 x 128 x 32] remain the same.

- Down sampling is done by the POOL 1 layer along the spatial dimensions (width, height), producing a volume of [64 x 64 x 32]. When the CONV2 layer computes, a volume with 32 filters, such as [64 x 64 x 32], is produced.
- The RELU2 layer applies an element-by-element activation function while maintaining the volume's original size [64 x 64 x 32].
- Down sampling is performed by POOL 2 layer, producing a volume that looks like [32 x 32 x 32].
- The CONV3 layer computes and generates a volume with 32 filters, such as [32x32 x 32].
- The RELU3 layer applies an element-by-element activation function while maintaining the volume's original size [32 x 32 x 32].
- Down sampling is performed by the POOL 3 layer, producing a volume that looks like [16 x 16 x 32].
- The FCRN classifier determines the score corresponding to image, yields a of size dimension [1 x 1 x 10]. Each of the ten values corresponding to a class score reflects the benign, malignant, and no cancer, respectively. Figure 5 shows a schematic diagram of the deep learning model of CNN with FCRN classifier.

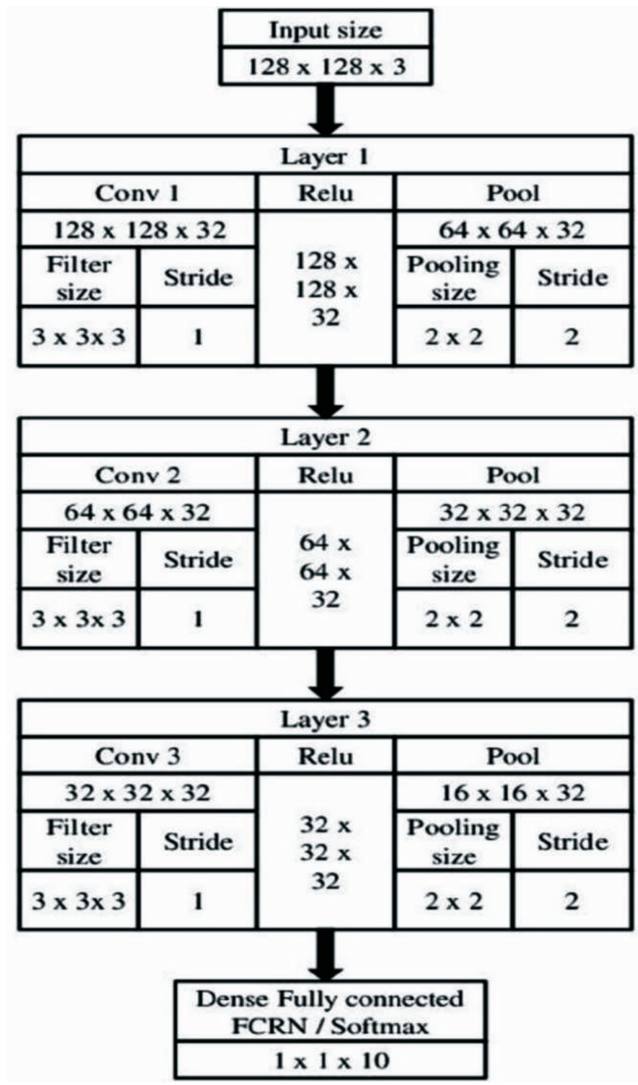

Figure 5. Schematic Diagram of DL-CNN with FCRN Classifier

2. Experimental Setup and Results Analysis

2.1 Dataset Collection

Due to privacy concerns, it is challenging to get genuine medical pictures for simulations. The Mammographic Image Analysis Society (MIAS), which has been used in the bulk of earlier research on the automated identification and categorization of breast cancer in mammographic images, provided the data collection that was used in this work. It comprises ground-truth marks from radiologists on the locations of the suspicious lesions and 322 digitalized film mammograms. The MIAS data is categorized using a variety of criteria, and the photographs categorized based on the severity of the irregularity are selected. Figure 6 shows benign and malignant lesions were also taken into consideration along with mammograms that did not reveal masses (Normal). The resolution of all the digitized photos is 128 x 128. They also include the locations of any potential problems. The information already available in the collection includes the abnormality's location, such as the center of a circle enclosing the tumor, its radius, the breast's position (left or right), the type of breast tissues, such as fatty, fatty-glandular, and dense, and the type of tumor, if any, that is present. In this work, 80% of data samples are considered for training dataset and 20% is used for testing purpose.

2.2 Results Analysis

Table 1 shows the obtained quality metrics of the proposed Level Set + GW-SVM classification approach

Method	Accuracy (in %)	Specificity (in %)	Sensitivity (in %)	F1-score
IRFRE (Wang et al., 2020b)	93	95	85	89.722
SAE + KNN (Adem, 2020)	91.24	89.05	92.98	90.972
TAN Bayes (Banu & Thirumalaikolundusubramanian, 2018)	94.11	93.4	95.2	94.291
Hough + SVM (Vijayarajeswari et al., 2019)	91.3	91.3	89.3	90.288
Proposed level set + GW-SVM	95.5	97	97	94.83

Table 1. Performance Metrics of the Proposed Level Set + GW-SVM Classification Model

and the various existing ML-based classification algorithms from the literature like IRFRE, SAE + KNN, TAN Bayes, and Hough + SVM, where IRFRE outperforms both the SAE + KNN and Hough + SVM approaches with 93% accuracy while TAN Bayes has slightly greater than IRFRE with 94.11% (Wang et al., 2020b; Adem, 2020; Banu & Thirumalaikolundusubramanian, 2018; Vijayarajeswari et al., 2019). However, proposed level set + GW-SVM classification obtained an improved accuracy and even other quality metrics like sensitivity, specificity and F1-score since the model utilized the unified set of features obtained from C-V level set and GW filter. Therefore, it has rendered the better performance over existing ML-based classification models for the detection of breast cancer form mammogram images. Further, graphical representation of performance comparison of level set + GW-SVM classification model with existing ML-based approaches is shown in Figure 7.

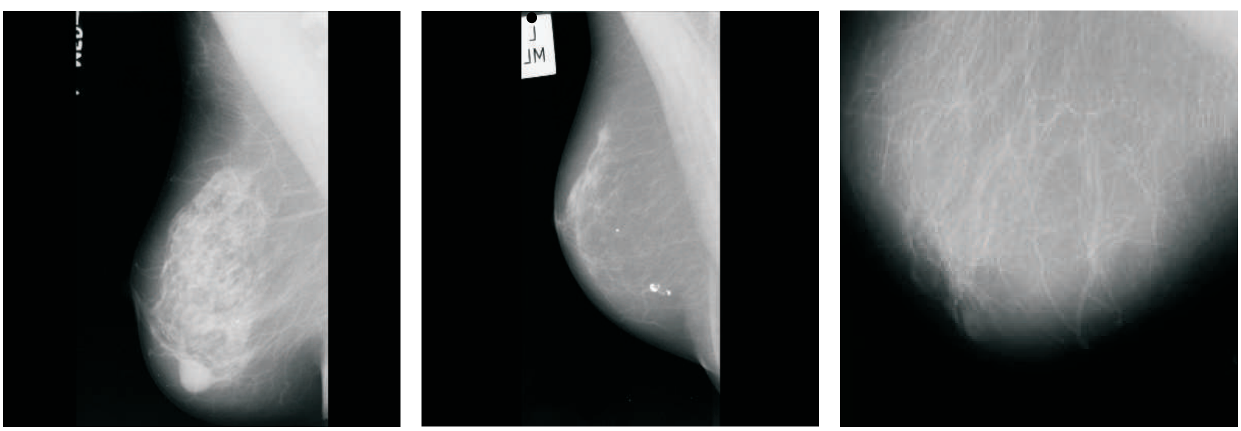

(a) (b) (c)

Figure 6. Sample Dataset Images (a) Benign (b) Malignant (c) Normal

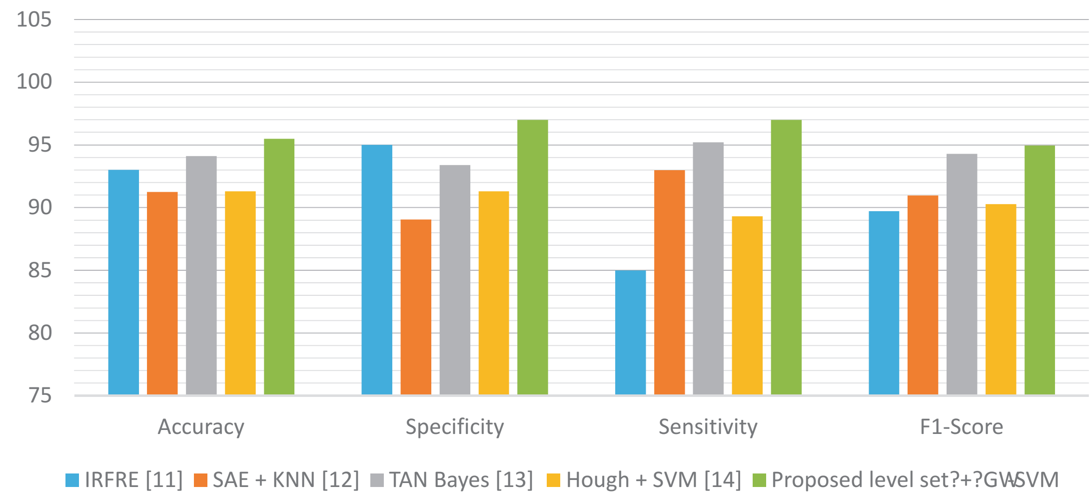

Figure 7. Performance Comparison of Proposed Level Set + GW-SVM Classification Model

$$\text{F1 Score} = 2 * \frac{\text{precision} * \text{Recall}}{\text{precision} + \text{Recall}}$$

$$\text{Accuracy} = \frac{\text{TP} + \text{TN}}{\text{TP} + \text{FP} + \text{TN} + \text{FN}}$$

Table 2 shows the obtained quality metrics performance using the proposed Chan-Vese + GW-DL-CNN with FCRN classifier and existing DL-based CAD systems like ANN, CNNI-BCC, CNN model + NN, and C-V + DL-CNN + NN for the detection and classification of breast cancer in mammogram images. The proposed Level Set + GW-DL-CNN with FCRN classifier obtained enhanced accuracy of 98.6% and even other quality metrics like specificity, sensitivity, and F1-score, respectively, as compared to existing DL-based approaches in the literature, since the proposed Level Set + GW-DL-CNN with FCRN classifier method utilized the hybrid combinations of features learning with FCRN classification (Kaymak et al., 2017; Ting et al., 2019; Duraisamy & Emperumal, 2017).

Method	Accuracy (in %)	Specificity (in %)	Sensitivity (in %)	F1-score
ANN (Kaymak et al., 2017)	70.4	-	-	80.78
CNNI-BCC (Ting et al., 2019)	90.50	90.71	89.47	90.085
DL-CNN + NN (Duraisamy & Emperumal, 2017)	91	80	93.75	92.71
Level set + DL-CNN + NN (Duraisamy & Emperumal, 2017)	96	90	97.5	94
Proposed level set + GW-DL-CNN-FCRN	98.6	98	98	97.08

Table 2. Performance Evaluation of the Proposed C-V + GW-DL-CNN Integrated with the FCRN Classifier

Further, the performance comparison of accuracy and F1-score obtained using proposed level set + GW-DI-CNN with FCRN classifier model as compared to the existing DL-based approaches is closed in Figure 8, while Figure 9 depicts the performance of specificity and sensitivity of

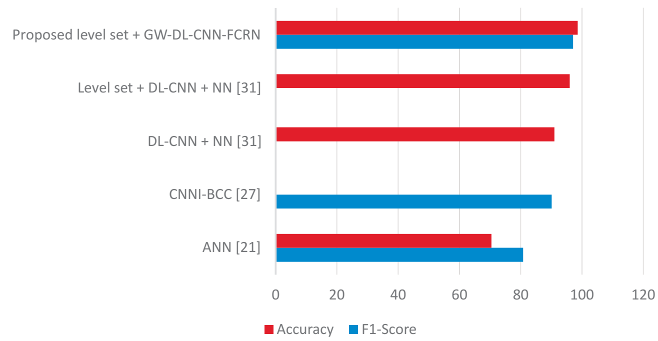

Figure 8. Performance Comparison of Accuracy and F1-score Using Proposed C-V + GW-DL-CNN with FCRN Classifier Model with Existing DL-based Approaches

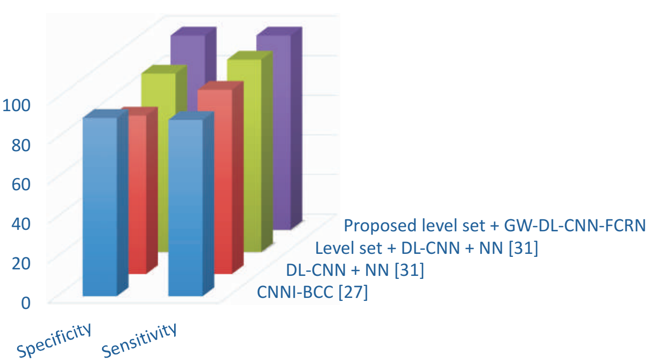

Figure 9. Performance Comparison of Specificity and Sensitivity of Proposed C-V + GW-DL-CNN with FCRN Classifier Model and Existing DL-based Approaches

proposed C-V + DL-CNN with FCRN classifier model and existing deep learning-based approaches.

Conclusion

This study proposes a Computer-Aided Diagnosis (CAD) system based on a hybrid intelligence framework utilizing GW-DL-CNN for the detection and classification of breast cancer in mammographic images. Additionally, a machine learning framework incorporating GW-SVM is also implemented. Furthermore, Chan-Vese (C-V) feature-based level set segmentation is employed to segment objects with poorly defined boundaries in mammographic images. The unified features extracted from both C-V and GW filters are fed into SVM and the DL-CNN with an FCRN classifier to classify breast cancer into categories such as malignant, benign, or normal. The classification performance is evaluated on standard benchmark datasets, and extensive results show that the proposed Level Set + GW-SVM classifier and C-V + GW-DL-CNN with FCRN classifier significantly outperform traditional machine learning and deep learning-based approaches in the literature, based on quality metrics such as accuracy, specificity, sensitivity, and F1-score. Future research could explore the integration of additional advanced quantum machine learning techniques to further improve classification accuracy and processing efficiency. Expanding the dataset to include diverse mammographic images from various demographics could enhance the model's generalization. Moreover, integrating real-time processing capabilities with edge devices for on-site breast cancer detection in clinical settings is a promising direction.

References

[1]. Adem, K. (2020). Diagnosis of breast cancer with Stacked autoencoder and Subspace kNN. *Physica A: Statistical Mechanics and its Applications,* 551, 124591.

https://doi.org/10.1016/j.physa.2020.124591

[2]. Banu, B., & Thirumalaikolundusubramanian, P. (2018). Comparison of Bayes classifiers for breast cancer classification. *Asian Pacific Journal of Cancer Prevention (APJCP),* 19(10), 2917.

https://doi.org/10.22034/APJCP.2018.19.10.2917

[3]. Bilalović, O., & Avdagić, Z. (2018). Robust breast cancer classification based on GA optimized ANN and ANFIS-voting structures. In 2018 *41st International Convention on Information and Communication Technology, Electronics and Microelectronics (MIPRO)* (pp. 0279-0284). IEEE.

https://doi.org/10.23919/MIPRO.2018.8400053

[4]. Budak, Ü., Cömert, Z., Rashid, Z. N., Şengür, A., & Çıbuk, M. (2019). Computer-aided diagnosis system combining FCN and Bi-LSTM model for efficient breast cancer detection from histopathological images. *Applied Soft Computing,* 85, 105765.

https://doi.org/10.1016/j.asoc.2019.105765

[5]. Chavez, T., Vohra, N., Wu, J., Bailey, K., & El-Shenawee, M. (2019). Breast cancer detection with low-dimensional ordered orthogonal projection in terahertz imaging. *IEEE Transactions on Terahertz Science and Technology*, 10(2), 176-189.

https://doi.org/10.1109/TTHZ.2019.2962116

[6]. Duraisamy, S., & Emperumal, S. (2017). Computer-aided mammogram diagnosis system using deep learning convolutional fully complex valued relaxation neural network classifier. *IET Computer Vision,* 11(8), 656-662.

https://doi.org/10.1049/iet-cvi.2016.0425

[7]. Eltrass, A. S., & Salama, M. S. (2020). Fully automated scheme for computer-aided detection and breast cancer diagnosis using digitised mammograms. *IET Image Processing,* 14(3), 495-505.

https://doi.org/10.1049/iet-ipr.2018.5953

[8]. Hu, H. (2020). Segmentation of breast mass and diagnosis of benign and malignant breast tumors based on edge constraint in pulse coupled neural network. *Journal of Medical Imaging and Health Informatics,* 10(7), 1597-1602.

https://doi.org/10.1166/jmihi.2020.3086

[9]. Huang, Q., Chen, Y., Liu, L., Tao, D., & Li, X. (2019). On combining biclustering mining and AdaBoost for breast tumor classification. *IEEE Transactions on Knowledge and*

Data Engineering, 32(4), 728-738.

https://doi.org/10.1109/TKDE.2019.2891622

[10]. Ibrahim, A., Mohammed, S., Ali, H. A., & Hussein, S. E. (2020). Breast cancer segmentation from thermal images based on chaotic salp swarm algorithm. *IEEE Access,* 8, 122121-122134.

https://doi.org/10.1109/ACCESS.2020.3007336

[11]. Kaymak, S., Helwan, A., & Uzun, D. (2017). Breast cancer image classification using artificial neural networks. *Procedia Computer Science,* 120, 126-131.

https://doi.org/10.1016/j.procs.2017.11.219

[12]. Li, T., & Fong, S. (2023). Similarity measure of breast cancer datasets using fuzzy rule-based classification by attribute. In *Research Anthology on Medical Informatics in Breast and Cervical Cancer* (pp. 247-265). IGI Global.

https://doi.org/10.4018/978-1-6684-7136-4.ch014

[13]. Lotfi, E., & Keshavarz, A. (2014). Gene expression microarray classification using PCA–BEL. *Computers in Biology and Medicine,* 54, 180-187.

https://doi.org/10.1016/j.compbiomed.2014.09.008

[14]. Melinda, V., Primartha, R., Wijaya, A., & Jambak, M. I. (2020). Optimization Naïve Bayes algorithm using particle swarm optimization in the classification of breast cancer. In *Sriwijaya International Conference on Information Technology and Its Applications (SICONIAN 2019)* (pp. 362-369). Atlantis Press.

https://doi.org/10.2991/aisr.k.200424.055

[15]. Mojrian, S., Pinter, G., Joloudari, J. H., Felde, I., Szabo-Gali, A., Nadai, L., & Mosavi, A. (2020). Hybrid machine learning model of extreme learning machine radial basis function for breast cancer detection and diagnosis; A multilayer fuzzy expert system. In 2020 *RIVF International Conference on Computing and Communication Technologies (RIVF)* (pp. 1-7). IEEE.

https://doi.org/10.1109/RIVF48685.2020.9140744

[16]. Nahid, A. A., Mehrabi, M. A., & Kong, Y. (2018). Histopathological breast cancer image classification by deep neural network techniques guided by local clustering. *BioMed Research International,* 2018(1), 2362108.

https://doi.org/10.1155/2018/2362108

[17]. Pérez, M., Benalcázar, M. E., Tusa, E., Rivas, W., & Conci, A. (2017). Mammogram classification using back-propagation neural networks and texture feature descriptors. In 2017 *IEEE Second Ecuador Technical Chapters Meeting (ETCM)* (pp. 1-6). IEEE.

https://doi.org/10.1109/ETCM.2017.8247515

[18]. Roslidar, R., Rahman, A., Muharar, R., Syahputra, M. R., Arnia, F., Syukri, M., & Munadi, K. (2020). A review on recent progress in thermal imaging and deep learning approaches for breast cancer detection. *IEEE Access,* 8, 116176-116194.

https://doi.org/10.1109/ACCESS.2020.3004056

[19]. Sayed, G. I., Darwish, A., & Hassanien, A. E. (2020). Binary whale optimization algorithm and binary moth flame optimization with clustering algorithms for clinical breast cancer diagnoses. *Journal of Classification,* 37(1), 66-96.

https://doi.org/10.1007/s00357-018-9297-3

[20]. Sebai, M., Wang, T., & Al-Fadhli, S. A. (2020). PartMitosis: A partially supervised deep learning framework for mitosis detection in breast cancer histopathology images. *IEEE Access,* 8, 45133-45147.

https://doi.org/10.1109/ACCESS.2020.2978754

[21]. Sujatha, K., Durgadevi, G., Kumar, K. S., Karthikeyan, V., Ponmagal, R. S., Hari, R., & Cao, S. Q. (2020). Screening and early identification of microcalcifications in breast using texture-based ANFIS classification. In *Wearable and Implantable Medical Devices* (pp. 115-140). Academic Press.

https://doi.org/10.1016/B978-0-12-815369-7.00005-7

[22]. Thangavel, K., & Kaja Mohideen, A. (2016). Mammogram classification using ANFIS with ant colony optimization based learning. In *Digital Connectivity–Social Impact: 51st Annual Convention of the Computer Society of India, CSI 2016, Coimbatore, India, December 8-9, 2016, Proceedings 51* (pp. 141-152). Springer Singapore.

https://doi.org/10.1007/978-981-10-3274-5_12

[23]. Ting, F. F., Tan, Y. J., & Sim, K. S. (2019). Convolutional neural network improvement for breast cancer classification. *Expert Systems with Applications,* 120, 103-115.

https://doi.org/10.1016/j.eswa.2018.11.008

[24]. Utami, D. A., & Rustam, Z. (2019). Gene selection in cancer classification using hybrid method based on Particle Swarm Optimization (PSO), Artificial Bee Colony (ABC) feature selection and support vector machine. In *AIP Conference Proceedings,* 2168, 020047. AIP Publishing.

https://doi.org/10.1063/1.5132474

[25]. Valkonen, M., Isola, J., Ylinen, O., Muhonen, V., Saxlin, A., Tolonen, T., & Ruusuvuori, P. (2019). Cytokeratin-supervised deep learning for automatic recognition of epithelial cells in breast cancers stained for ER, PR, and Ki-67. *IEEE Transactions on Medical Imaging,* 39(2), 534-542.

https://doi.org/10.1109/TMI.2019.2933656

[26]. Vijayarajeswari, R., Parthasarathy, P., Vivekanandan, S., & Basha, A. A. (2019). Classification of mammogram for early detection of breast cancer using SVM classifier and Hough transform. *Measurement,* 146, 800-805

https://doi.org/10.1016/j.measurement.2019.05.083

[27]. Wang, L., Shen, H., Zhang, J., Zhu, Y., & Jiang, C. (2019). A clifford analytic signal-based breast lesion segmentation method for 4D spatial-temporal DCE-MRI sequences. *IEEE Access,* 8, 3901-3910.

https://doi.org/10.1109/ACCESS.2019.2962750

[28]. Wang, S., Wang, Y., Wang, D., Yin, Y., Wang, Y., & Jin, Y. (2020b). An improved random forest-based rule extraction method for breast cancer diagnosis. *Applied Soft Computing,* 86, 105941.

https://doi.org/10.1016/j.asoc.2019.105941

[29]. Wang, Y., Lei, B., Elazab, A., Tan, E. L., Wang, W., Huang, F., & Wang, T. (2020a). Breast cancer image classification via multi-network features and dual-network orthogonal low-rank learning. *IEEE Access*, 8, 27779-27792.

https://doi.org/10.1109/ACCESS.2020.2964276

[30]. Yao, H., Zhang, X., Zhou, X., & Liu, S. (2019). Parallel structure deep neural network using CNN and RNN with an attention mechanism for breast cancer histology image classification. *Cancers,* 11(12), 1901.

https://doi.org/10.3390/cancers11121901

[31]. Zheng, J., Lin, D., Gao, Z., Wang, S., He, M., & Fan, J. (2020). Deep learning assisted efficient AdaBoost algorithm for breast cancer detection and early diagnosis. *Ieee Access,* 8, 96946-96954.

https://doi.org/10.1109/ACCESS.2020.2993536

ABOUT THE AUTHORS

Ongole Gandhi is currently pursuing his Ph.D. as a research scholar in the Department of Computer Science and Engineering at Jawaharlal Nehru Technological University, Kakinada, Andhra Pradesh, India. His research interests include Data Mining, Machine Learning, Deep Learning, and High-Performance Computing.

Dr. S. N. Tirumala Rao is a Professor and Head of the Department of Computer Science and Engineering at Narasaraopeta Engineering College, Narasaraopet, Andhra Pradesh, India. He has valuable professional experience spanning over two successful decades. Out of his 21 years of experience, he has spent 13 years in the teaching profession, while the remaining 8 years include experience and insights from the research industry. He has published a good number of papers in reputed journals. His research interests include Data Mining, Parallel Programming, and Computer Networks.

Dr. Munaga H. M. Krishna Prasad is currently a Full Professor in the Department of Computer Science and Engineering at the University College of Engineering Kakinada (A), Jawaharlal Nehru Technological University Kakinada (JNTUK), and also serves as Director (i/c), Internal Quality Assurance Cell, Jawaharlal Nehru Technological University, Kakinada, Andhra Pradesh. He has published over 75 research papers in various international journals and conferences, and has attended numerous national and international conferences in India and abroad. His research interests include Data Mining, Machine Learning, Big Data Analytics, and High-Performance Computing.